

Reference Correlations of the Thermal Conductivity of Cyclopentane, *iso*-Pentane, and *n*-Pentane

Cite as: J. Phys. Chem. Ref. Data **44**, 033102 (2015); <https://doi.org/10.1063/1.4927095>
Submitted: 14 May 2015 . Accepted: 06 July 2015 . Published Online: 13 August 2015

C.-M. Vassiliou, M. J. Assael, M. L. Huber, and R. A. Perkins



View Online



Export Citation



CrossMark

ARTICLES YOU MAY BE INTERESTED IN

Reference Correlation of the Viscosity of Toluene from the Triple Point to 675 K and up to 500 MPa

Journal of Physical and Chemical Reference Data **44**, 033101 (2015); <https://doi.org/10.1063/1.4926955>

Reference Correlation of the Thermal Conductivity of Carbon Dioxide from the Triple Point to 1100 K and up to 200 MPa

Journal of Physical and Chemical Reference Data **45**, 013102 (2016); <https://doi.org/10.1063/1.4940892>

Reference Correlations of the Thermal Conductivity of Ethene and Propene

Journal of Physical and Chemical Reference Data **45**, 033104 (2016); <https://doi.org/10.1063/1.4958984>

Where in the **world** is AIP Publishing?
Find out where we are exhibiting next



Reference Correlations of the Thermal Conductivity of Cyclopentane, *iso*-Pentane, and *n*-Pentane

C.-M. Vassiliou and M. J. Assael^{a)}

Laboratory of Thermophysical Properties and Environmental Processes, Chemical Engineering Department, Aristotle University, Thessaloniki 54636, Greece

M. L. Huber and R. A. Perkins

Applied Chemicals and Materials Division, National Institute of Standards and Technology, 325 Broadway, Boulder, Colorado 80305, USA

(Received 14 May 2015; accepted 6 July 2015; published online 13 August 2015)

New, wide-range reference equations for the thermal conductivity of cyclopentane, *iso*-pentane, and *n*-pentane are presented. The equations are based in part upon a body of experimental data that has been critically assessed for internal consistency and for agreement with theory whenever possible. In the case of the dilute-gas thermal conductivity, a theoretically based correlation was adopted in order to extend the temperature range of the experimental data. In the critical region, the enhancement of the thermal conductivity is well represented by theoretically based equations containing just one adjustable parameter, estimated by a predictive scheme. The thermal-conductivity equations behave in a physically reasonable manner over a wide range of conditions that correspond to the range of validity of the most accurate equations of state for each fluid. The estimated uncertainties of the correlations are dependent on the availability of accurate experimental data for validation, and are different for each fluid, varying from 1% (at the 95% confidence level) for the liquid phase of *iso*-pentane over the temperature range $307\text{ K} < T < 355\text{ K}$ at pressures up to 400 MPa (where high-accuracy data are available) to a more typical 4% for the liquid phase of cyclopentane over the temperature range $218\text{ K} < T < 240\text{ K}$ at pressures to 250 MPa. Estimated uncertainties in the gas phase are typically on the order of 3%–5%. For all three fluids, uncertainties in the critical region are much larger, since the thermal conductivity approaches infinity at the critical point and is very sensitive to small changes in density. © 2015 by the U.S. Secretary of Commerce on behalf of the United States. All rights reserved. [<http://dx.doi.org/10.1063/1.4927095>]

Key words: critical phenomena; cyclopentane; *iso*-pentane; *n*-pentane; reference correlations; thermal conductivity; transport properties.

CONTENTS

1. Introduction.....	2	3.2. The correlation for <i>iso</i> -pentane	7
2. Methodology	3	3.2.1. The dilute-gas limit of <i>iso</i> -pentane ...	8
2.1. The dilute-gas limit	3	3.2.2. The residual and the critical-enhancement contributions of <i>iso</i> -pentane	10
2.2. The residual thermal conductivity	4	3.3. The correlation for <i>n</i> -pentane	11
2.3. The critical enhancement	4	3.3.1. The dilute-gas limit of <i>n</i> -pentane ...	13
3. Thermal-Conductivity Correlations	4	3.3.2. The residual and the critical-enhancement contributions of <i>n</i> -pentane	13
3.1. The correlation for cyclopentane	4	4. Conclusion	15
3.1.1. The dilute-gas limit of cyclopentane .	5	Acknowledgment	16
3.1.2. The residual and the critical-enhancement contributions of cyclopentane	6	5. References	16

List of Tables

1. Thermal-conductivity measurements of cyclopentane	4
--	---

^{a)}Author to whom correspondence should be addressed; Electronic mail: assael@auth.gr.
© 2015 by the U.S. Secretary of Commerce on behalf of the United States. All rights reserved.

ethanol,⁹ and *ortho*-xylene, *meta*-xylene, *para*-xylene, and ethylbenzene,¹⁰ covering a wide range of conditions of temperature and pressure, were reported. In this paper, the work is extended to the thermal conductivity of cyclopentane, *iso*-pentane, and *n*-pentane.

The goal of this work is to critically assess the available literature data and provide wide-ranging correlations for the thermal conductivity of cyclopentane, *iso*-pentane, and *n*-pentane, that are valid over gas, liquid, and supercritical states, and incorporate densities provided by the recent equation of state of Gedanitz *et al.*¹¹ for cyclopentane, and the equations of state of Lemmon and Span¹² and Span and Wagner¹³ for *iso*-pentane and *n*-pentane, respectively. It was decided to treat the three compounds in one paper, since they are quite similar in their thermophysical properties, and are often found together.

2. Methodology

The thermal conductivity λ is expressed as the sum of three independent contributions, as

$$\lambda(\rho, T) = \lambda_o(T) + \Delta\lambda(\rho, T) + \Delta\lambda_c(\rho, T), \quad (1)$$

where ρ is the density, T is the temperature, and the first term, $\lambda_o(T) = \lambda(0, T)$, is the contribution to the thermal conductivity in the dilute-gas limit, where only two-body molecular interactions occur. The final term, $\Delta\lambda_c(\rho, T)$, the critical enhancement, arises from the long-range density fluctuations that occur in a fluid near its critical point, which contribute to divergence of the thermal conductivity at the critical point. Finally, the term $\Delta\lambda(\rho, T)$, the residual property, represents the contribution of all other effects to the thermal conductivity of the fluid at elevated densities.

The identification of these three separate contributions to the thermal conductivity and to transport properties in general is useful because it is possible, to some extent, to treat both $\lambda_o(T)$ and $\Delta\lambda_c(\rho, T)$ theoretically. In addition, it is possible to derive information about $\lambda_o(T)$ from experiment. In contrast, there is almost no theoretical guidance concerning the residual contribution, $\Delta\lambda(\rho, T)$, so its evaluation is based entirely on experimentally obtained data.

The analysis described above should be applied to the best available data for the thermal conductivity. Thus, a prerequisite to the analysis is a critical assessment of the experimental data. For this purpose, two categories of experimental data are defined: primary data employed in the development of the correlation, and secondary data used simply for comparison purposes. According to the recommendation adopted by the Subcommittee on Transport Properties (now known as The International Association for Transport Properties) of the International Union of Pure and Applied Chemistry, the primary data are identified by a well-established set of criteria.¹⁴ These criteria have been successfully employed to establish standard reference values for the viscosity and thermal conductivity of fluids over wide ranges of conditions, with uncertainties in the range of 1%. However, in many cases, such a narrow definition unacceptably limits the range of the data representation. Consequently, within the primary data

set, it is also necessary to include results that extend over a wide range of conditions, albeit with a poorer accuracy, provided they are consistent with other more accurate data or with theory. In all cases, the accuracy claimed for the final recommended data must reflect the estimated uncertainty in the primary information.

2.1. The dilute-gas limit

In order to be able to extrapolate the temperature range of the measurements, a theoretically based scheme was preferred to correlate the dilute-gas limit thermal conductivity, $\lambda_o(T)$, over a wide temperature range. The traditional kinetic approach for thermal conductivity results in an expression involving three generalized cross sections.^{15,16} However, it is possible to derive an equivalent kinetic theory expression for thermal conductivity by the approach of Thijssse *et al.*¹⁷ and Millat *et al.*,¹⁸ where one considers expansion in terms of total energy, rather than separating translational from internal energy as is done traditionally. In this case, the dilute-gas limit thermal conductivity, $\lambda_o(T)$ (mW m⁻¹ K⁻¹), of a polyatomic gas can be shown to be inversely proportional to a single generalized cross section,¹⁵⁻¹⁸ $S(10E)$, as

$$\lambda_o(T) = 1000 \frac{5k_B^2(1+r^2)T}{2m\langle v \rangle_o S(10E)} f_\lambda, \quad (2)$$

where k_B is the Boltzmann constant, T (K) is the absolute temperature, f_λ (-) is the dimensionless higher-order correction factor, m (kg) is the molecular mass, and $\langle v \rangle_o = 4\sqrt{k_B T / \pi m}$ (m/s) is the average relative thermal speed. The quantity r^2 is defined by $r^2 = 2C_{\text{int}}^o / 5k_B$, where C_{int}^o is the contribution of both the rotational, C_{rot}^o , and the vibrational, C_{vib}^o , degrees of freedom to the isochoric ideal heat capacity C_v^o .

The recent classical trajectory calculations¹⁹⁻²¹ confirm that, for most molecules studied, the higher-order thermal-conductivity correction factor is near unity. One can take advantage of this finding to define the effective generalized cross section $S_\lambda (= S(10E) / f_\lambda)$ (nm²), and rewrite Eq. (2) for the dilute-gas limit thermal conductivity, $\lambda_o(T)$ (mW m⁻¹ K⁻¹), as

$$\lambda_o(T) = C_\lambda \frac{(C_p^o / k_B) \sqrt{T}}{S_\lambda}, \quad (3)$$

where C_λ is a constant obtained from the molecular mass and Eq. (2) for each fluid, and the ideal-gas isobaric heat capacity, $C_p^o (= C_{\text{int}}^o + 2.5 k_B)$ in J/K, can be obtained from the literature.

It has been previously noted,¹⁸ and recently confirmed¹⁶ for smaller molecules, that the cross section $S(10E)$ exhibits a nearly linear dependence on the inverse temperature. Hence, experimental data will be employed to obtain coefficients a_0 and a_1 in

$$S_\lambda = a_0 + a_1 / T. \quad (4)$$

Although the scheme described by Eqs. (3) and (4) is strictly valid for smaller molecules, it has been found to work very well as a correlation tool for larger molecules.^{4,5,7,9} Hence, Eqs. (3) and (4) form a consistent set of equations for the calculation of the dilute-gas limit thermal conductivity.

2.2. The residual thermal conductivity

The thermal conductivities of pure fluids exhibit an enhancement over a large range of densities and temperatures around the critical point and become infinite at the critical point. This behavior can be described by models that produce a smooth crossover from the singular behavior of the thermal conductivity asymptotically close to the critical point to the residual values far away from the critical point.^{22–24} The density-dependent terms for thermal conductivity can be grouped according to Eq. (1) as $[\Delta\lambda(\rho, T) + \Delta\lambda_c(\rho, T)]$. To assess the critical enhancement theoretically, we need to evaluate, in addition to the dilute-gas thermal conductivity, the residual thermal-conductivity contribution. The procedure adopted for this analysis used ODRPACK (Ref. 25) to fit all the primary data simultaneously to the residual thermal conductivity and the critical enhancement, while maintaining the values of the dilute-gas thermal-conductivity already obtained. The density values employed were obtained by the equation of state of Gledhill *et al.*¹¹ for cyclopentane, of Lemmon and Span¹² for *iso*-pentane, and of Span and Wagner¹³ for *n*-pentane. The primary data were weighted in inverse proportion to the square of their uncertainty.

The residual thermal conductivity was represented with a polynomial in temperature and density,

$$\Delta\lambda(\rho, T) = \sum_{i=1}^5 (B_{1,i} + B_{2,i}(T/T_c)) (\rho/\rho_c)^i. \quad (5)$$

Coefficients $B_{1,i}$ and $B_{2,i}$ will be obtained for each fluid separately employing the corresponding primary data.

2.3. The critical enhancement

The theoretically based crossover model proposed by Olchowy and Sengers^{22–24} is complex and requires solution of a quartic system of equations in terms of complex variables. A simplified crossover model has also been proposed by Olchowy and Sengers.²⁶ The critical enhancement of the thermal conductivity from this simplified model is given by

$$\Delta\lambda_c = \frac{\rho C_p R_D k_B T}{6\pi\bar{\eta}\xi} (\bar{\Omega} - \bar{\Omega}_0), \quad (6)$$

with

$$\bar{\Omega} = \frac{2}{\pi} \left[\left(\frac{C_p - C_v}{C_p} \right) \arctan(\bar{q}_D \xi) + \frac{C_v}{C_p} \bar{q}_D \xi \right] \quad (7)$$

and

$$\bar{\Omega}_0 = \frac{2}{\pi} \left[1 - \exp \left(- \frac{1}{(\bar{q}_D \xi)^{-1} + (\bar{q}_D \xi \rho_c / \rho)^2 / 3} \right) \right]. \quad (8)$$

In Eqs. (6)–(8), k_B is Boltzmann's constant, $\bar{\eta}$ is the viscosity, and C_p and C_v are the isobaric and isochoric specific heat obtained from the literature for each fluid. The correlation length ξ is given by

$$\xi = \xi_0 \left(\frac{p_c \rho}{\Gamma \rho_c^2} \right)^{\nu/\gamma} \left[\left. \frac{\partial \rho(T, \rho)}{\partial p} \right|_T - \left(\frac{T_{\text{ref}}}{T} \right) \left. \frac{\partial \rho(T_{\text{ref}}, \rho)}{\partial p} \right|_T \right]^{\nu/\gamma}. \quad (9)$$

In the above equations for the three fluids studied, values for the universal constants $R_D = 1.02$, $\nu = 0.63$, and $\gamma = 1.239$ were employed using a universal representation of the critical enhancement of the thermal conductivity (based on a simplified solution of mode-coupling theory with fluid-specific parameters determined by a corresponding-states method) by Perkins *et al.*²⁷ Furthermore, since for these three fluids very few data exist in the critical region, we employ the same method presented by Perkins *et al.*²⁷ to predict the effective cutoff wavelength \bar{q}_D^{-1} as well as the system-dependent amplitude Γ and ξ_0 , and the reference temperature T_{ref} .

3. Thermal-Conductivity Correlations

3.1. The correlation for cyclopentane

Table 1 summarizes, to the best of our knowledge, the experimental measurements of the thermal conductivity of cyclopentane reported in the literature. From the nine sets shown in the table, six were considered as primary data.

The measurements of Assael and Dalaouti³⁰ were obtained in absolute transient hot-wire instruments employing two anodized Ta wires, with uncertainties of 0.5% based on a full theoretical model proven to operate with such an uncertainty. Measurements performed by the group of Assael

TABLE 1. Thermal-conductivity measurements of cyclopentane

First author	Year of publication	Technique employed ^a	Purity (%)	Uncertainty (%)	No. of data	Temperature range (K)	Pressure range (MPa)
Primary data							
Watanabe ²⁸	2004	THW	98	0.4	15	257–317	0.1
Marrucho ^{29,b}	2003	THW	na	3	4	353–413	0.1
Assael ³⁰	2001	THW	99.5	0.5	41	234–308	0.1–16.2
Heinemann ^{31,b}	2000	THW	na	1	3	335–418	0.1
Grigor'ev ³²	1981	CC	na	1.5	56	295–455	0.1–150
Andersson ³³	1978	THW	99	na	32	218–274	18–250 ^c
Secondary data							
Takada ^{34,b}	1998	CC	99	4	1	343	0.1
Sakiadis ³⁵	1957	PP	99	1	9	293–320	0.1
Lambert ^{36,b}	1955	THW	99.4	0.5	1	339	0.1

^aCC, coaxial cylinder; na, not available; PP, parallel plate; THW, transient hot wire.

^bIncludes vapor data employed to derive the dilute-gas thermal-conductivity correlation.

^cRestricted to 250 MPa (restriction imposed by the pressure limit of the equation of state¹¹).

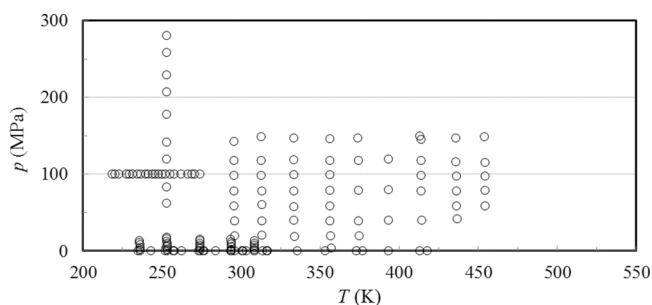


FIG. 1. Temperature-pressure ranges of the primary experimental thermal conductivity data for cyclopentane.

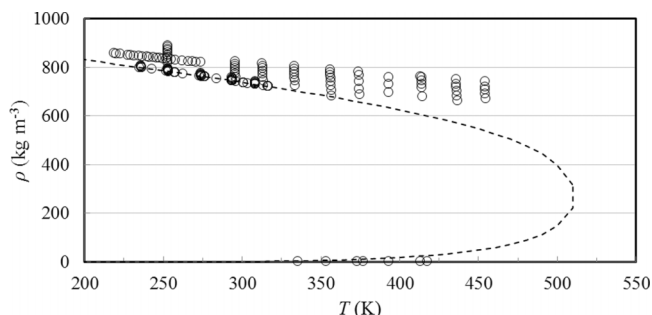


FIG. 2. Temperature-density ranges of the primary experimental thermal conductivity data for cyclopentane. (---) saturation curve.

have been successfully employed in many thermal-conductivity reference correlations.^{1,2,4-9} The measurements of Watanabe and Kato²⁸ were also performed in an absolute transient hot-wire instrument, with an uncertainty of 0.4%. Measurements of these investigators have also been employed in previous thermal-conductivity reference correlations.⁴⁻⁷ Hence, these two sets were considered as primary data.

Heinemann *et al.*³¹ and Marrucho *et al.*²⁹ employed the same transient hot-wire instrument with two platinum wires to measure the thermal conductivity of gases and vapors with a respective uncertainty of 1% and 3%. These measurements, backed by full theory, were also included in the primary dataset. The measurements of Grigor'ev and Ishkhanov³² were performed in a concentric-cylinder instrument with an uncertainty of 1.5%. Measurements performed by this group have successfully been employed in previous thermal-conductivity reference correlations,^{1,3,4} and are therefore considered as primary data. Finally, the transient hot-wire measurements of Andersson³³ were also included in the primary data set, with a lower weight, as they extended the temperature and pressure

range of application of the correlation. The remaining data were categorized as secondary data.

Figures 1 and 2 show the ranges of the primary measurements outlined in Table 1; the saturation curve may be seen in Fig. 2. As already mentioned, the critical enhancement term will be calculated theoretically; the lack of data in that region can be seen in Fig. 2. Temperatures for all data were converted to the ITS-90 temperature scale.³⁷ The development of the correlation requires densities; Gedanitz *et al.*¹¹ recently reviewed the thermodynamic properties of cyclopentane and developed an accurate, wide-ranging equation of state valid for single-phase and saturation states from the triple point (179.7 K) to 550 K at pressures up to 250 MPa, with an expanded uncertainty in density of 0.2% in the liquid phase, and up to 1% above the critical region. We also adopt their values for the critical temperature, T_c , the critical density, ρ_c , and the triple-point temperature, as 511.72 K, 274.921 kg m⁻³, and 179.7 K, respectively. Finally, as already mentioned, the isobaric ideal-gas heat capacity was obtained from the same source.¹¹

3.1.1. The dilute-gas limit of cyclopentane

Substituting in Eq. (2) the molecular mass [(0.070 132 9/6.022 14 × 10²³) kg] of cyclopentane, Eq. (3) becomes

$$\lambda_0(T) = 6.661\,238 \times 10^{-2} \frac{(C_p^0/k_B) \sqrt{T}}{S_\lambda}. \quad (10)$$

The isobaric heat capacity, $C_p^0 (=C_{\text{int}}^0 + 2.5 k_B)$, can be obtained from Gedanitz *et al.*¹¹ as

$$\frac{C_p^0}{k_B} = \nu_0 + \sum_{i=1}^4 \nu_i \left(\frac{u_i}{T} \right)^2 \frac{\exp(u_i/T)}{[\exp(u_i/T) - 1]^2}, \quad (11)$$

where $\nu_0 = 4.0$, $\nu_1 = 1.34$, $\nu_2 = 13.4$, $\nu_3 = 17.4$, $\nu_4 = 6.65$, $u_1 = 230$ K, $u_2 = 1180$ K, $u_3 = 2200$ K, and $u_4 = 5200$ K.

Of the primary measurements shown in Table 1, only Marrucho *et al.*²⁹ and Heinemann *et al.*³¹ performed measurements near the dilute-gas limit. Hence, data from the secondary sets of Takada *et al.*³⁴ and Lambert *et al.*³⁶ were also considered for the correlation in the dilute-gas limit. These measurements were employed, together with Eqs. (10) and (11), to obtain the coefficients a_0 and a_1 of Eq. (4), as

$$S_\lambda = 0.3637 + 201.58/T. \quad (12)$$

Equations (10)–(12) form a consistent set of equations for the calculation of the dilute-gas limit thermal conductivity of cyclopentane.

The values of the dilute-gas limit thermal conductivity, $\lambda_0(T)$ in mW m⁻¹ K⁻¹, obtained by the scheme of Eqs. (10)–(12), were fitted as a function of the reduced temperature $T_r = T/T_c$ for ease of use to the following equation:

$$\lambda_0(T) = \frac{-8.252\,334\,6 + 76.336\,54 T_r - 217.6154 T_r^2 + 312.298\,77 T_r^3}{1 + 0.283\,414\,79 T_r + 2.789\,054\,1 T_r^2 + 0.326\,450\,05 T_r^3}. \quad (13)$$

Values calculated by Eq. (13) do not deviate from the values calculated by the scheme of Eqs. (10)–(12) by more than 0.2% over the temperature range from 180 K to 1000 K. Equation (13) is hence employed in the calculations that will follow.

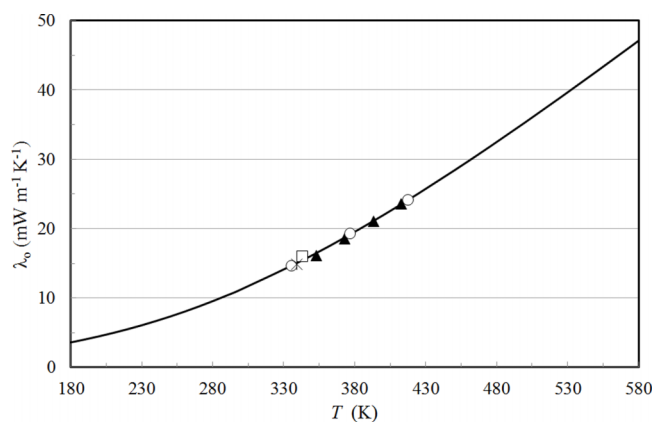


FIG. 3. Dilute-gas thermal conductivity of cyclopentane as a function of temperature. Marrucho *et al.*²⁹ (\blacktriangle), Heinemann *et al.*³¹ (\circ), Takada *et al.*³⁴ (\square), Lambert *et al.*³⁶ (\ast), values calculated by Eq. (13) (—).

Figure 3 shows the dilute-gas thermal-conductivity values of the selected investigators, and the values calculated by Eqs. (10)–(12), as a function of the temperature. In Fig. 4, percentage deviations of the dilute-gas thermal conductivity of cyclopentane from the scheme of Eqs. (10)–(12) are also shown. They all agree with the present correlation within a maximum deviation of 3.7%. Based on these measurements, the uncertainty of the correlation, at the 95% confidence level over the temperature range 330 K–430 K, is 2.8%. The correlation behaves in a physically reasonable manner over the entire range from the triple point to 550 K (the limit of the equation of state); however, we anticipate the uncertainty may be larger in the areas where data are unavailable and the correlation is extrapolated.

3.1.2. The residual and the critical-enhancement contributions of cyclopentane

As already mentioned, the coefficients $B_{1,i}$ and $B_{2,i}$ in Eq. (5) were fitted with ODRPACK (Ref. 25) to the primary data for the thermal conductivity of cyclopentane. The crossover model requires the system-dependent amplitudes Γ and ξ_0 .

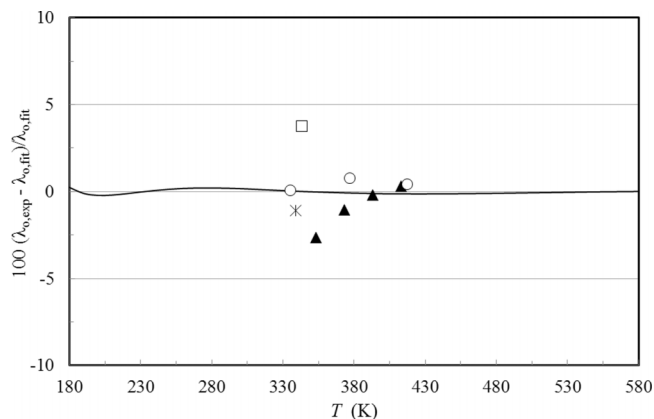


FIG. 4. Percentage deviations of the dilute-gas thermal conductivity of cyclopentane from the scheme of Eqs. (10)–(12). Marrucho *et al.*²⁹ (\blacktriangle), Heinemann *et al.*³¹ (\circ), Takada *et al.*³⁴ (\square), Lambert *et al.*³⁶ (\ast), values calculated by Eq. (13) (—).

TABLE 2. Coefficients of Eq. (5) for the residual thermal conductivity of cyclopentane

i	$B_{1,i}$ (mW m ⁻¹ K ⁻¹)	$B_{2,i}$ (mW m ⁻¹ K ⁻¹)
1	$9.205\,36 \times 10^{-2}$	$-4.351\,29 \times 10^{-2}$
2	$-1.726\,99 \times 10^{-1}$	$1.126\,36 \times 10^{-1}$
3	$1.265\,57 \times 10^{-1}$	$-9.086\,63 \times 10^{-2}$
4	$-3.622\,96 \times 10^{-2}$	$2.809\,50 \times 10^{-2}$
5	$3.887\,18 \times 10^{-3}$	$-2.803\,68 \times 10^{-3}$

For this work, we adopted the value $\Gamma = 0.058$ and estimated $\xi_0 = 2.16 \times 10^{-10}$ m, using a universal representation of the critical enhancement of the thermal conductivity (based on a simplified solution of mode-coupling theory with fluid-specific parameters determined by a corresponding-states method) by Perkins *et al.*²⁷ Furthermore, since no data exist in the critical region, see Fig. 2, we used this same method²⁷ to estimate the effective cutoff wavelength \bar{q}_D^{-1} and found it equal to 6.24×10^{-10} m. The viscosity required for Eq. (6) was estimated by an extended corresponding-states method of Huber *et al.*³⁸ The reference temperature T_{ref} , far above the critical temperature where the critical enhancement is negligible, was calculated by $T_{\text{ref}} = (3/2) T_c$,³⁹ which for cyclopentane is 767.58 K. The coefficients $B_{1,i}$ and $B_{2,i}$ of Eq. (5) obtained are shown in Table 2.

Table 3 summarizes comparisons of the primary data with the correlation. We have defined the percentage deviation as $\text{PCTDEV} = 100 * (\lambda_{\text{exp}} - \lambda_{\text{fit}}) / \lambda_{\text{fit}}$, where λ_{exp} is the experimental value of the thermal conductivity and λ_{fit} is the value calculated from the correlation. Thus, the average absolute percentage deviation (AAD) is found with the expression $\text{AAD} = (\sum |\text{PCTDEV}|) / n$, where the summation is over all n points, and the bias percent is $\text{BIAS} = (\sum \text{PCTDEV}) / n$. We estimate the uncertainty (at the 95% confidence level) for the thermal conductivity in the liquid state down to 240 K to be 2.4%, rising to 4% for lower temperatures. For the dilute gas, over the temperature range 330 K–430 K, we estimate the uncertainty to be 2.8%. Uncertainties in the critical region are much larger, since the thermal conductivity approaches infinity at the critical point and is very sensitive to small changes in density. In addition, due to lack of data above 455 K, it is difficult to assess the uncertainty; however, the correlation behaves in a physically reasonable manner up to the limit of validity of the equation of state of Gleditsch *et al.*,¹¹ 550 K.

Figure 5 shows the percentage deviations of all primary thermal-conductivity data from the values calculated by

TABLE 3. Evaluation of the cyclopentane thermal-conductivity correlation for the primary data

First author	Year of publication	AAD (%)	BIAS (%)
Watanabe ²⁸	2004	0.23	−0.21
Marrucho ²⁹	2003	3.55	−3.55
Assael ³⁰	2001	0.23	0.03
Heinemann ³¹	2000	2.44	−2.44
Grigor'ev ³²	1981	0.46	−0.21
Andersson ³³	1978	2.69	0.78
Entire data set		1.19	−0.02

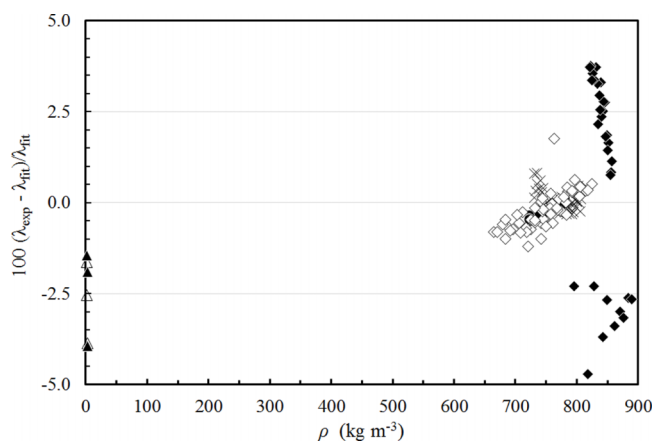


FIG. 5. Percentage deviations of primary experimental data of cyclopentane from the values calculated by the present model, Eqs. (1), (5)–(9), and (13), as a function of density. Watanabe and Kato²⁸ (●), Marrucho *et al.*²⁹ (Δ), Assael and Dalaouti³⁰ (×), Heinemann *et al.*³¹ (▲), Andersson³³ (◆), Grigor'ev and Ishkhanov³² (◇).

Eqs. (1), (5)–(9), and (13), as a function of the density. The lack of experimental data in the critical region is apparent. Figures 6 and 7 show the same deviations, but as a function of the temperature and pressure, respectively.

Table 4 shows the average absolute percentage deviation (AAD) and the bias for the secondary data. Finally, Figs. 8 and 9 show the thermal conductivity of cyclopentane as a function of the temperature for different pressures, and as a function of the density for different temperatures. The theoretically predicted values of the thermal conductivity around and above the critical point are shown.

In Table 5, recommended values for the thermal conductivity are given. For checking computer implementations of the correlation, a point is provided for testing code with critical enhancement at 512.0 K and 400.0 kg m⁻³ (5.0512 MPa), where the thermal conductivity is 69.698 mW m⁻¹ K⁻¹; the dilute-gas thermal conductivity, $\lambda_o(512 \text{ K}) = 37.042 \text{ mW m}^{-1} \text{ K}^{-1}$, the residual term

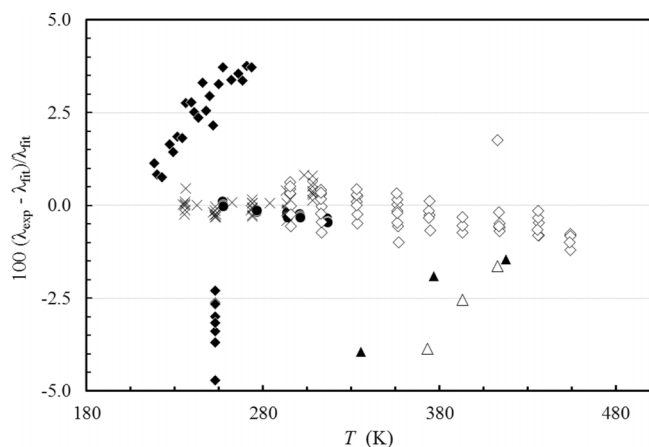


FIG. 6. Percentage deviations of primary experimental data of cyclopentane from the values calculated by the present model, Eqs. (1), (5)–(9), and (13), as a function of temperature. Watanabe and Kato²⁸ (●), Marrucho *et al.*²⁹ (Δ), Assael and Dalaouti³⁰ (×), Heinemann *et al.*³¹ (▲), Andersson³³ (◆), Grigor'ev and Ishkhanov³² (◇).

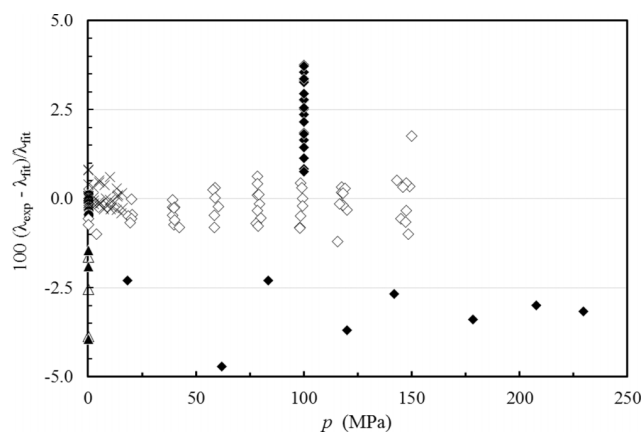


FIG. 7. Percentage deviations of primary experimental data of cyclopentane from the values calculated by the present model, Eqs. (1), (5)–(9), and (13), as a function of pressure. Watanabe and Kato²⁸ (●), Marrucho *et al.*²⁹ (Δ), Assael and Dalaouti³⁰ (×), Heinemann *et al.*³¹ (▲), Andersson³³ (◆), Grigor'ev and Ishkhanov³² (◇).

TABLE 4. Evaluation of the cyclopentane thermal-conductivity correlation for the secondary data

First author	Year of publication	AAD (%)	BIAS (%)
Takada ³⁴	1998	0.01	-0.01
Sakiadis ³⁵	1957	3.42	-3.42
Lambert ³⁶	1955	5.10	5.10

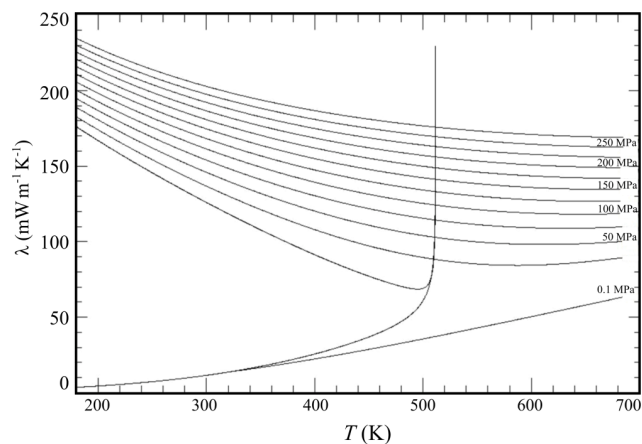


FIG. 8. Thermal conductivity of cyclopentane as a function of temperature for different pressures.

$\Delta\lambda(400.0 \text{ kg m}^{-3}, 512 \text{ K}) = 24.018 \text{ mW m}^{-1} \text{ K}^{-1}$, and the critical enhancement term, $\Delta\lambda(400.0 \text{ kg m}^{-3}, 512 \text{ K}) = 8.638 \text{ mW m}^{-1} \text{ K}^{-1}$. The viscosity used in the calculation of the enhancement for this state point is 40.842 $\mu\text{Pa s}$.

3.2. The correlation for *iso*-pentane

Table 6 summarizes, to the best of our knowledge, the experimental measurements of the thermal conductivity of *iso*-pentane reported in the literature. From the eleven sets shown in the table, four were considered as primary data.

The measurements of Al-Harbi *et al.*⁴¹ were obtained in an absolute transient hot-wire instrument employing two anodized Ta wires, with uncertainties of 0.3% based on a full theoretical model proven to operate with such an

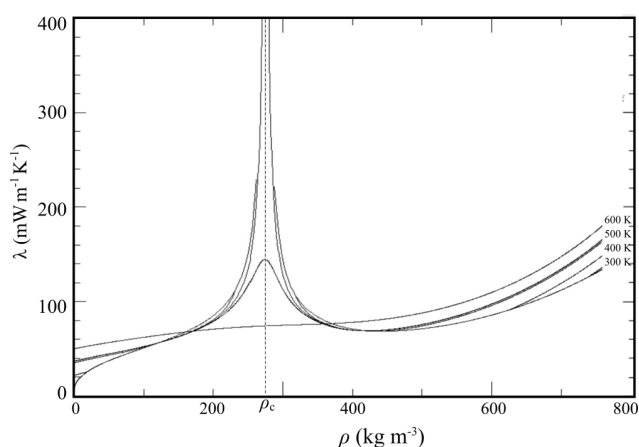


FIG. 9. Thermal conductivity of cyclopentane as a function of density for different temperatures.

uncertainty. Measurements performed by this group (headed by Wakeham) have been successfully employed in many thermal-conductivity reference correlations.^{2,4–7,10}

Heinemann *et al.*³¹ and Dohrn *et al.*⁴⁰ employed the same transient hot-wire instrument with two platinum wires to measure the thermal conductivity of gases and vapors with a respective uncertainty of 1% and 3%. These measurements, backed by full theory, were also employed successfully in the reference correlation of the thermal conductivity of cyclopentane, and thus they are included in the primary data. Finally, the measurements of Senftleben,⁴² performed in a hot-wire instrument with an uncertainty extending to 2%, were also included in the primary data set, as they extend to higher temperatures. The remaining data were categorized as secondary data.

Figures 10 and 11 show the ranges of the primary measurements outlined in Table 6; the saturation curve can be seen in Fig. 11. As already mentioned, the critical enhancement term will be calculated theoretically; the lack of data in that region can be seen in Fig. 11. Temperatures for all data were converted to the ITS-90 temperature scale.³⁷ The development of the correlation requires densities; Lemmon and Span¹² reviewed the thermodynamic properties of *iso*-pentane and developed

TABLE 5. Recommended values of cyclopentane thermal conductivity ($\text{mW m}^{-1} \text{K}^{-1}$)

Pressure (MPa)	Temperature (K)			
	200	300	400	500
0	4.489	11.25	21.94	35.32
0.1	166.8	125.9	22.39	35.62
50		145.8	120.2	104.0
100		161.3	139.3	125.3
150		174.6	154.9	142.3
200		186.5	168.6	157.1
250			180.9	170.4

an accurate, wide-ranging equation of state valid for single-phase and saturation states from the triple point (112.65 K) to 500 K at pressures up to 1000 MPa. The uncertainties are approximately 0.2% in density at temperatures up to 320 K, 0.5% in density at higher temperatures, 2% in heat capacity above 250 K, 4% in heat capacity at lower temperatures with an expanded uncertainty of 0.2% in the liquid phase, and up to 1% above the critical region. We also adopt their values for the critical temperature, T_c , and the critical density, ρ_c , as 460.35 K and 236.0 kg m^{-3} , respectively. Finally, as already mentioned, the isobaric ideal-gas heat capacity was obtained from the same source.¹²

3.2.1. The dilute-gas limit of *iso*-pentane

Substituting in Eq. (2) the molecular mass $[(0.072\,148\,78/6.022\,14 \times 10^{23}) \text{ kg}]$ of *iso*-pentane, Eq. (3) becomes

$$\lambda_o(T) = 6.567\,509 \times 10^{-2} \frac{(C_p^o/k_B) \sqrt{T}}{S_\lambda}. \quad (14)$$

The isobaric heat capacity, $C_p^o (=C_{\text{int}}^o + 2.5 k_B)$, can be obtained from Lemmon and Span¹² as

$$\frac{C_p^o}{k_B} = v_0 + \sum_{i=1}^4 v_i \left(\frac{u_i}{T} \right)^2 \frac{\exp(u_i/T)}{[\exp(u_i/T) - 1]^2}, \quad (15)$$

TABLE 6. Thermal-conductivity measurements of *iso*-pentane

First author	Year of publication	Technique employed ^a	Purity (%)	Uncertainty (%)	No. of data	Temperature range (K)	Pressure range (MPa)
Primary data							
Dohrn ^{40,b}	2007	THW	>99	3	12	343–391	0.1–0.5
Heinemann ^{31,b}	2000	THW	na	1	4	354–391	0.1
Al-Harbi ⁴¹	1991	THW	>99	0.3	43	307–355	32–406
Senftleben ^{42,b}	1964	HW	na	1–2	8	273–673	0.03–0.7
Secondary data							
Parkinson ^{43,b}	1972	THW	99	2	2	323, 373	0.1
Vilcu ^{44,b}	1972	THW	na	na	4	323–357	0.1
Filippov ⁴⁵	1968	CC	na	3	7	283–300	0.1
Vilim ⁴⁶	1960	CC	na	2	1	293	0.1
Sakiadis ³⁵	1957	PP	99	1	10	302–323	0.1–0.2
Lambert ^{36,b}	1955	THW	99.4	0.5	1	339	0.1
Moser ⁴⁷	1913	na	na	na	5	273–457	0.03–0.1

^aCC, coaxial cylinder; na, not available; HW, hot wire; PP, parallel plate; THW, transient hot wire.

^bIncludes vapor data employed to derive the dilute-gas thermal-conductivity correlation.

where $v_0 = 4.0$, $v_1 = 7.4056$, $v_2 = 9.5772$, $v_3 = 15.765$, $v_4 = 12.119$, $u_1 = 442$ K, $u_2 = 1109$ K, $u_3 = 2069$ K, and $u_4 = 4193$ K.

Of the primary measurements shown in Table 6, only Dohrn *et al.*,⁴⁰ Heinemann *et al.*,³¹ and Senftleben⁴² performed measurements near the dilute-gas limit. Hence, data from the secondary sets of Parkinson and Gray,⁴³ Vilcu and Ciochina,⁴⁴ and Lambert *et al.*³⁶ were also considered for the correlation in the dilute-gas limit. These measurements were employed, together with Eqs. (14) and (15), to obtain the coefficients a_0

and a_1 of Eq. (4), as

$$S_k = 0.2325 + 265.63/T. \quad (16)$$

Equations (14)–(16) form a consistent set of equations for the calculation of the dilute-gas limit thermal conductivity of *iso*-pentane.

The values of the dilute-gas limit thermal conductivity, $\lambda_0(T)$ in $\text{mW m}^{-1} \text{K}^{-1}$, obtained by the scheme of Eqs. (14)–(16), were fitted as a function of the reduced temperature $T_r = T/T_c$ for ease of use to the following equation:

$$\lambda_0(T) = \frac{0.773\,049 - 15.9754\,T_r + 218.987\,T_r^2 - 329.556\,T_r^3 + 281.075\,T_r^4 + 53.326\,T_r^5}{5.104\,67 - 8.120\,44\,T_r + 8.116\,07\,T_r^2 - 0.294\,969\,T_r^3 + T_r^4}. \quad (17)$$

Values calculated by Eq. (17) do not deviate from the values calculated by the scheme of Eqs. (10)–(12) by more than 0.05% over the temperature range from 113 K to 1000 K. Equation (17) is hence employed in the calculations that will follow.

Figure 12 shows the dilute-gas thermal conductivity values of the selected investigators, and the values calculated by Eqs. (14)–(16), as a function of the temperature. In Fig. 13, percentage deviations of the dilute-gas thermal conductivity of *iso*-pentane from the scheme of Eqs. (14)–(16) are also shown. Based on these measurements, the estimated uncertainty of the correlation, at the 95% confidence level, over the temperature range 273 K–673 K, is 4.5%. The correlation behaves in

a physically reasonable manner over the extrapolated range down to the triple point; however, we anticipate the uncertainty may be larger as the triple point is approached.

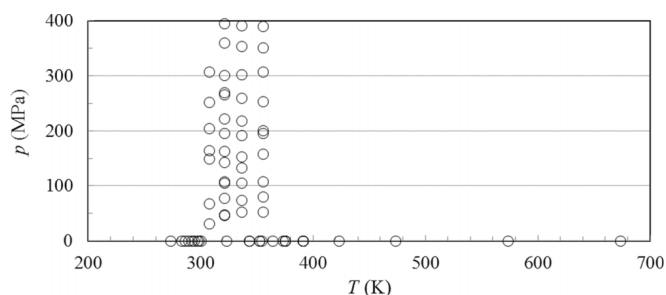


FIG. 10. Temperature-pressure ranges of the primary experimental thermal-conductivity data for *iso*-pentane.

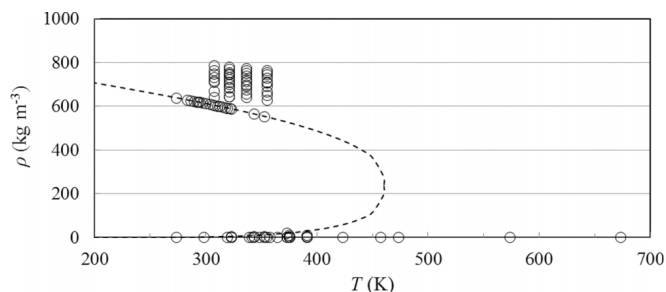


FIG. 11. Temperature-density ranges of the primary experimental thermal-conductivity data for *iso*-pentane. (---) saturation curve.

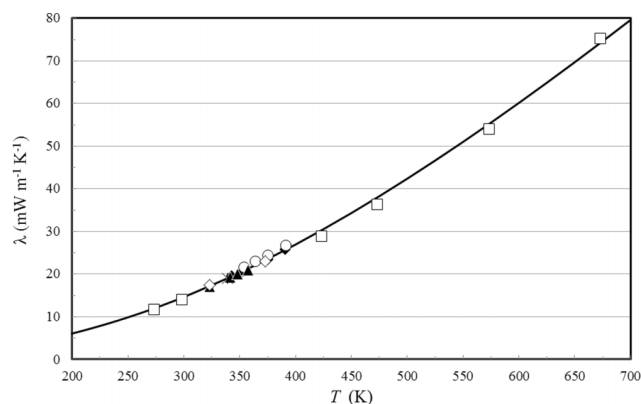


FIG. 12. Dilute-gas thermal conductivity of *iso*-pentane as a function of temperature. Dohrn *et al.*⁴⁰ (◆), Heinemann *et al.*³¹ (○), Vilcu and Ciochina⁴⁴ (▲), Parkinson and Gray⁴³ (◇), Senftleben⁴² (□), Lambert *et al.*³⁶ (*), values calculated by Eq. (17) (—).

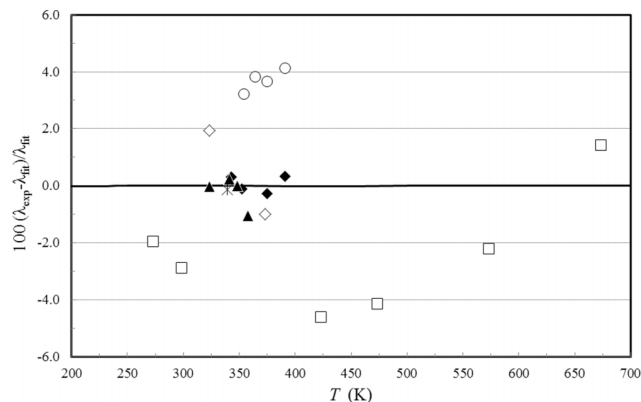


FIG. 13. Percentage deviations of the dilute-gas thermal conductivity of *iso*-pentane from the scheme of Eqs. (14)–(16). Dohrn *et al.*⁴⁰ (◆), Heinemann *et al.*³¹ (○), Vilcu and Ciochina⁴⁴ (▲), Parkinson and Gray⁴³ (◇), Senftleben⁴² (□), Lambert *et al.*³⁶ (*), values calculated by Eq. (17) (—).

TABLE 7. Coefficients of Eq. (5) for the residual thermal conductivity of *iso*-pentane

i	$B_{1,i}$ (mW m ⁻¹ K ⁻¹)	$B_{2,i}$ (mW m ⁻¹ K ⁻¹)
1	$-1.175\,07 \times 10^1$	$5.140\,03 \times 10^0$
2	$-1.613\,46 \times 10^1$	$5.584\,45 \times 10^1$
3	$5.272\,54 \times 10^1$	$-9.514\,74 \times 10^1$
4	$-2.749\,40 \times 10^1$	$4.752\,68 \times 10^1$
5	$4.548\,17 \times 10^0$	$-7.292\,96 \times 10^0$

3.2.2. The residual and the critical-enhancement contributions of *iso*-pentane

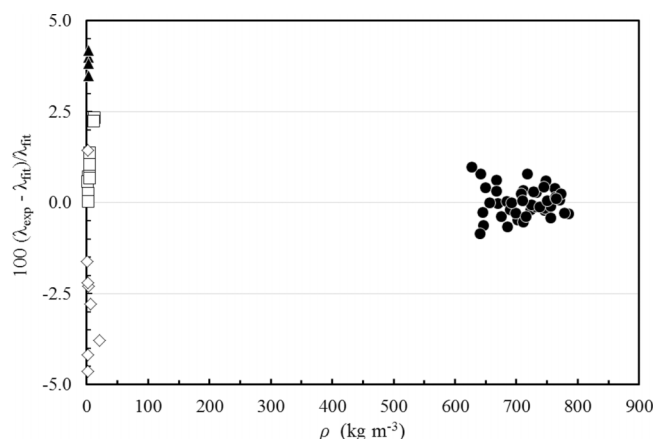
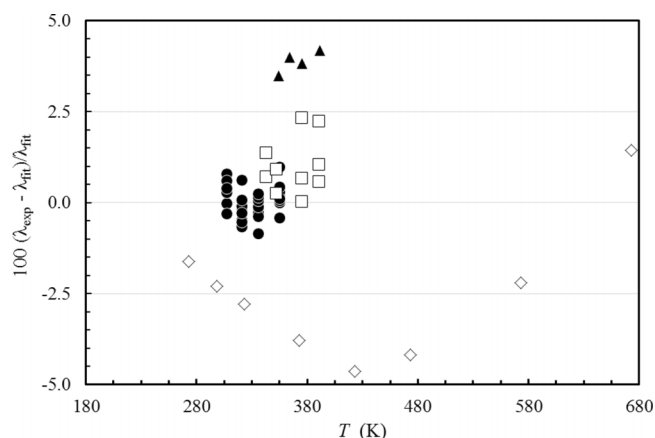
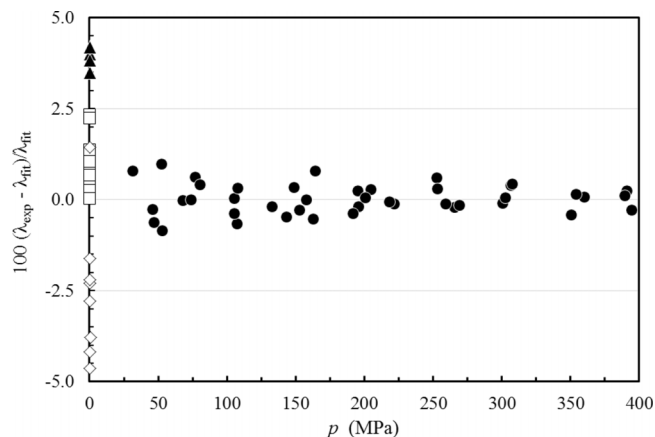
As already mentioned, the coefficients $B_{1,i}$ and $B_{2,i}$ in Eq. (5) were fitted with ODRPACK (Ref. 25) to the primary data for the thermal conductivity of *iso*-pentane. As was done for cyclopentane, we used the theoretically based model of Perkins *et al.*²⁷ to obtain the system-dependent amplitudes Γ and ξ_0 , which were found to be $\Gamma = 0.058$ and $\xi_0 = 2.27 \times 10^{-10}$ m, and again, due to lack of experimental data in the critical region, estimated the effective cutoff wavelength \bar{q}_D^{-1} to be 6.64×10^{-10} m. The viscosity required for Eq. (6) was obtained by REFPROP v9.1 (Ref. 48). The reference temperature T_{ref} was calculated by $T_{\text{ref}} = (3/2) T_c$,³⁹ which for *iso*-pentane is 690.53 K. The coefficients $B_{1,i}$ and $B_{2,i}$ of Eq. (5) obtained are shown in Table 7.

Table 8 summarizes comparisons of the primary data with the correlation. We estimate the uncertainty (at the 95% confidence level) for the thermal conductivity in the liquid state from 307 K to 355 K at pressures to 400 MPa to be 1%. However, this is a somewhat small temperature range and unfortunately high-quality dense-fluid data are unavailable outside of this range. Based on our experience with other fluids, we estimate that the uncertainty in the liquid and supercritical region is on the order of 4%–5%, and the correlation behaves in a physically reasonable manner over the range of applicability of the equation of state of Lemmon and Span.¹² For the thermal conductivity of the dilute gas, over the temperature range 273 K to 673 K, we estimate the uncertainty to be 4.5%. Future measurements should be made over a wider range of temperatures (above 355 K and below 307 K) to allow more thorough validation of this correlation, or the development of a new one if necessary. Additional gas-phase measurements are also desirable, since there is considerable scatter in the present data as shown in Fig. 13.

Figure 14 shows the percentage deviations of all primary thermal-conductivity data from the values calculated by Eqs. (1), (5)–(9), and (17), as a function of the density. The lack of experimental data in the critical region is apparent.

TABLE 8. Evaluation of the *iso*-pentane thermal-conductivity correlation for the primary data

First author	Year of publication	AAD (%)	BIAS (%)
Dohrn ⁴⁰	2007	1.00	1.00
Heinemann ³¹	2000	3.88	3.88
Al-Harbi ⁴¹	1991	0.32	0.001
Senftleben ⁴²	1964	2.87	−2.51
Entire data set		0.97	0.05

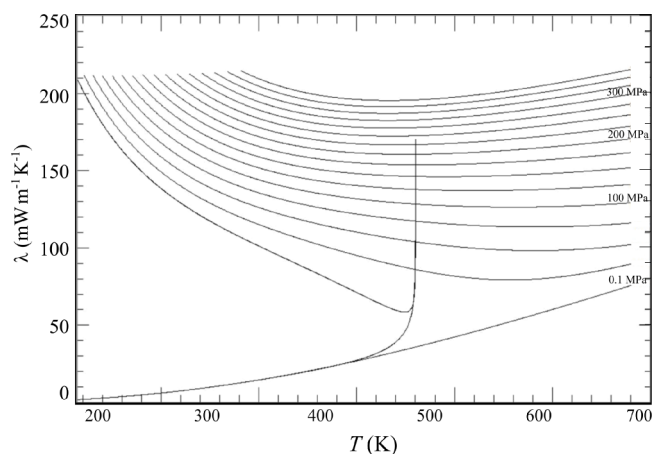
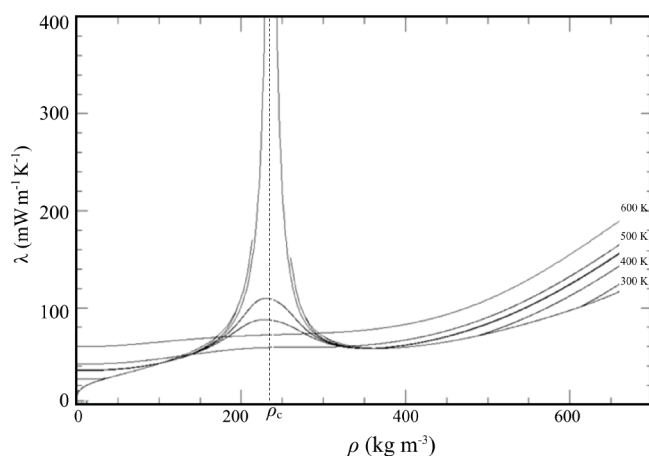
FIG. 14. Percentage deviations of primary experimental data of *iso*-pentane from the values calculated by the present model, Eqs. (1), (5)–(9), and (17), as a function of density. Dohrn *et al.*⁴⁰ (□), Heinemann *et al.*³¹ (▲), Senftleben⁴² (◇), Al-Harbi *et al.*⁴¹ (●).FIG. 15. Percentage deviations of primary experimental data of *iso*-pentane from the values calculated by the present model, Eqs. (1), (5)–(9), and (17), as a function of temperature. Dohrn *et al.*⁴⁰ (□), Heinemann *et al.*³¹ (▲), Senftleben⁴² (◇), Al-Harbi *et al.*⁴¹ (●).FIG. 16. Percentage deviations of primary experimental data of *iso*-pentane from the values calculated by the present model, Eqs. (1), (5)–(9), and (17), as a function of pressure. Dohrn *et al.*⁴⁰ (□), Heinemann *et al.*³¹ (▲), Senftleben⁴² (◇), Al-Harbi *et al.*⁴¹ (●).

Figures 15 and 16 show the same deviations but as a function of the temperature and pressure, respectively.

Table 9 shows the average absolute percentage deviation (AAD) and the bias for the secondary data. Finally, Figs. 17

TABLE 9. Evaluation of the *iso*-pentane thermal-conductivity correlation for the secondary data

First author	Year of publication	AAD (%)	BIAS (%)
Parkinson ⁴³	1972	1.57	0.85
Vilcu ⁴⁴	1972	0.56	0.22
Filippov ⁴⁵	1968	9.15	9.15
Vilim ⁴⁶	1960	6.90	6.90
Sakiadis ³⁵	1957	8.37	8.37
Lambert ³⁶	1955	0.33	0.33
Moser ⁴⁷	1913	5.38	-4.50

FIG. 17. Thermal conductivity of *iso*-pentane as a function of temperature for different pressures.FIG. 18. Thermal conductivity of *iso*-pentane as a function of density for different temperatures.

and 18 show the thermal conductivity of *iso*-pentane as a function of the temperature for different pressures, and as a function of the density for different temperatures. The theoretically predicted values of the thermal conductivity around and at temperatures above the critical point are shown.

In Table 10, recommended values for the thermal conductivity are given. For checking computer implementations of the correlation, a point is provided for testing code with critical enhancement at 460 K and 329.914 kg m⁻³ (3.5 MPa), where the thermal conductivity is 59.649 mW m⁻¹ K⁻¹; the dilute-gas thermal conductivity, $\lambda_o(460 \text{ K}) = 35.883 \text{ mW m}^{-1} \text{ K}^{-1}$, the residual term $\Delta\lambda(329.914 \text{ kg m}^{-3}, 460 \text{ K}) = 14.321 \text{ mW m}^{-1} \text{ K}^{-1}$, and

TABLE 10. Recommended values of *iso*-pentane thermal conductivity (mW m⁻¹ K⁻¹)

Pressure (MPa)	Temperature (K)			
	200	300	400	500
0	6.1	14.6	26.9	42.3
0.1	138.5	101.1	26.9	42.3
50	158.8	126.1	110.1	100.8
100	176.5	144.0	131.7	127.0
150		158.9	148.0	146.0
200		172.0	161.4	161.2
250		183.7	172.9	173.7
300		194.5	183.0	184.3
400		214.1	200.0	201.3

the critical enhancement term, $\Delta\lambda(329.914 \text{ kg m}^{-3}, 460 \text{ K}) = 9.445 \text{ mW m}^{-1} \text{ K}^{-1}$. The viscosity used in the calculation of the enhancement for this state point is 36.170 $\mu\text{Pa s}$.

3.3. The correlation for *n*-pentane

Table 11 summarizes, to the best of our knowledge, the experimental measurements of the thermal conductivity of *n*-pentane reported in the literature. From the 30 sets shown in the table, 11 were considered as primary data.

The measurements of Palavra *et al.*⁵³ and Papadaki *et al.*⁵² were obtained in absolute transient hot-wire instruments employing two anodized Ta wires, with uncertainties of 0.3% based on a full theoretical model proven to operate with such an uncertainty. Measurements performed by this group (headed by Wakeham) have been successfully employed in many thermal-conductivity reference correlations.^{2,4-7,10} The measurements of Watanabe^{49,50} were also performed in an absolute transient hot-wire instrument, with an uncertainty of 0.5%. Measurements of this investigator have been employed successfully in the thermal-conductivity reference correlation of cyclopentane and also in previous thermal-conductivity reference correlations.⁴⁻⁷ Transient hot-wire instruments were also employed by Sun *et al.*⁵¹ and Kandiyoti *et al.*,⁵⁶ with uncertainties of 1% and 1.3%, respectively. The measurements of Sun *et al.*⁵¹ were successfully included in the thermal-conductivity reference correlation of toluene,⁴ while the measurements of Kandiyoti *et al.*⁵⁶ were included in the corresponding correlation for *n*-heptane.⁷ Thus, all the aforementioned measurements were included in the primary dataset.

Heinemann *et al.*³¹ and Dohrn *et al.*⁴⁰ employed the same transient hot-wire instrument with two platinum wires to measure the thermal conductivity of gases and vapors with a respective uncertainty of 1% and 3%. These measurements, backed by full theory, were also employed successfully in the reference correlation of the thermal conductivity of cyclopentane and *iso*-pentane. The measurements of Dohrn *et al.*⁴⁰ were thus considered as primary data. However, as will be shown in Sec. 3.3.2, the *n*-pentane measurements of Heinemann *et al.*³¹ are, for no apparent reason, about 10% higher than everybody else; hence, these were not included in the primary data. A hot-wire instrument was employed by Mukhamedzyanov *et al.*⁵⁷ for measurements to high pressures, with an uncertainty of 2%. Measurements

TABLE 11. Thermal-conductivity measurements of *n*-pentane

First author	Year of publication	Technique employed ^a	Purity (%)	Uncertainty (%)	No. of data	Temperature range (K)	Pressure range (MPa)
Primary data							
Dohrn ^{40,b}	2007	THW	>99	3	12	343–407	0.1–0.5
Watanabe ⁴⁹	2003	THW	98	0.5	1	298	0.101
Watanabe ⁵⁰	2002	THW	98	0.5	12	259–306	0.012–0.091
Sun ⁵¹	2002	THW	99.5	0.5	176	297–429	0.68–34.61
Papadaki ⁵²	1993	THW	99.9	1	1	306	0.091
Palavra ⁵³	1987	THW	99	0.3	58	306–359	1.8–70 ^c
Naziev ^{54,b}	1984	CC	na	2	18	373–624	0.1–2.0
Naziev ⁵⁵	1981	CC	na	1.5	42	174–287	0.1–50.0
Kandiyoti ⁵⁶	1972	THW	99.98	1.3	18	146–286	0–0.004
Mukhamedzyanov ⁵⁷	1971	HW	99.94	2	53	298–448	0.098–70 ^c
Brykov ⁵⁸	1970	CC	na	2	16	153–303	0.101
Secondary data							
Shi ⁵⁹	2006	THW	99.99	na	8	377–378	34.17
Heinemann ³¹	2000	THW	na	1	3	355–421	0.4–1.5
Rowley ⁶⁰	1987	THW	99.99	1	1	298	0.101
El-Sharkawy ⁶¹	1983	na	98.9	2.5	9	293–373	0.057–0.592
Bulanov ⁶²	1974	na	na	2	8	303–333	0.1–0.04
Mallan ⁶³	1972	THW	na	2.5	9	299–379	0.07–0.68
Bogotov ⁶⁴	1969	na	na	na	51	293–473	0.0098–49.0
Carmichael ^{65,b}	1969	CC	na	0.4	117	277–477	0.03–34.47
Pittman ⁶⁶	1968	THW	99.98	0.5	5	146–286	0.101
Jobst ⁶⁷	1964	na	na	2.0	9	183–303	0.101
Vilim ⁴⁶	1960	HW	na	2.0	2	293–309	0.101
Smith ^{68,b}	1960	CC	99.9	4.0	5	323–423	0.101
Lambert ^{36,b}	1955	THW	99.4	0.5	1	339	0.101
Bromley ^{69,b}	1952	na	na	4	1	293	0.06
Riedel ⁷⁰	1948	CC	99.99	na	1	293	0.101
Smith ⁷¹	1936	CC	na	na	2	303–333	0.08–0.21
Bridgman ⁷²	1923	CC	na	0.1	4	303–348	0–70 ^c
Moser ^{47,b}	1913	na	na	na	2	273–293	0.02–0.06
Goldschmidt ⁷³	1911	HW	na	na	4	194–273	0.101

^aCC, coaxial cylinder; na, not available; HW, hot wire; THW, transient hot wire.

^bIncludes vapor data employed to derive the dilute-gas thermal-conductivity correlation.

^cRestricted to 70 MPa (restriction imposed by the pressure limit of the equation of state).

of this investigator were successfully employed in previous thermal-conductivity reference correlations,^{6–9} and thus were included in the primary dataset.

Finally, a concentric-cylinder instrument was employed by Naziev *et al.*⁵⁴ at high temperatures, and by Naziev *et al.*⁵⁵ and Brykov *et al.*⁵⁸ at low temperatures, with uncertainties of less than 2%. Measurements of Naziev *et al.*^{54,55} were included in previous thermal-conductivity reference correlations,^{6–8,10} while those of Brykov *et al.*⁵⁸ were employed in the reference correlations of ethanol⁹ and ethylbenzene.¹⁰ These measurements also formed part of the primary dataset. The remaining data were categorized as secondary data.

Figures 19 and 20 show the ranges of the primary measurements outlined in Table 11; the saturation curve can be seen in Fig. 20. As already mentioned, the critical enhancement term will be calculated theoretically; the lack of data in that region can be seen in Fig. 20. Temperatures for all data were converted to the ITS-90 temperature scale.³⁷ The development of the correlation requires densities; Span and Wagner¹³ developed an accurate, wide-ranging equation of state valid for single-phase and saturation states from the triple point (143.47 K) to 600 K at pressures up to 70 MPa—this pressure limit also restricts the present thermal-conductivity correlation. The uncertainty in density is approximately 0.2%,

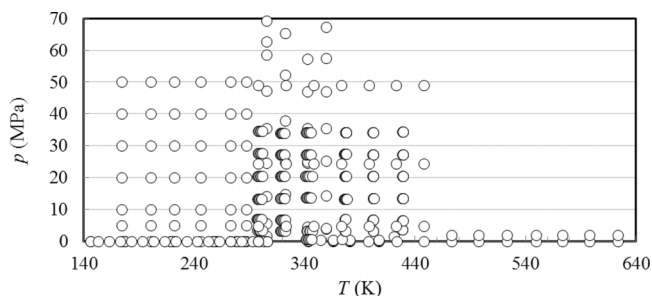


FIG. 19. Temperature-pressure ranges of the primary experimental thermal-conductivity data for *n*-pentane.

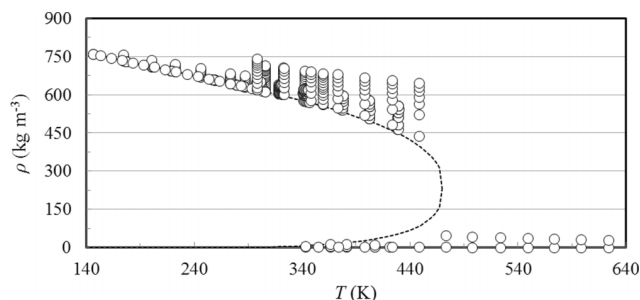


FIG. 20. Temperature-density ranges of the primary experimental thermal-conductivity data for *n*-pentane. (---) saturation curve.

rising to 0.5% at higher pressures. We also adopt their values for the critical temperature, T_c , and the critical density, ρ_c , as 469.7 K and 232.0 kg m⁻³, respectively. The isobaric ideal-gas heat capacity was obtained by Jaeschke and Schley,⁷⁴ valid over the temperature range 200–1000 K with an uncertainty of 0.5% rising to 1% at higher temperatures.

3.3.1. The dilute-gas limit of *n*-pentane

Substituting in Eq. (2) the molecular mass [(0.072 149/6.022 14 × 10²³) kg] of *n*-pentane, Eq. (3) becomes

$$\lambda_0(T) = 6.532\,926 \times 10^{-2} \frac{(C_p^0/k_B)\sqrt{T}}{S_\lambda}. \quad (18)$$

The isobaric heat capacity, $C_p^0 (=C_{\text{int}}^0 + 2.5 k_B)$, can be obtained from Jaeschke and Schley⁷⁴ as

$$\begin{aligned} \frac{C_p^0}{k_B} = & v_0 + v_1 \left\{ \frac{u_1/T}{\sinh(u_1/T)} \right\}^2 + v_2 \left\{ \frac{u_2/T}{\cosh(u_2/T)} \right\}^2 \\ & + v_3 \left\{ \frac{u_3/T}{\sinh(u_3/T)} \right\}^2, \end{aligned} \quad (19)$$

where $v_0 = 4.0$, $v_1 = 8.950\,43$, $v_2 = 21.8360$, $v_3 = 33.4032$, $u_1 = 178.670$ K, $u_2 = 840.538$ K, and $u_3 = 1774.25$ K.

Of the primary measurements shown in Table 11, only Dohrn *et al.*⁴⁰ and Naziev *et al.*⁵⁴ performed measurements near the dilute-gas limit. Hence, data from the secondary sets of Carmichael *et al.*,⁶⁵ Smith *et al.*,⁶⁸ Lambert *et al.*,³⁶ Bromley,⁶⁹ and Moser⁴⁷ were also considered for the correlation in the dilute-gas limit. We note that the lowest temperature point of Naziev *et al.*⁵⁴ was not considered, as it showed a deviation of more than 10% from all other points. These measurements were employed, together with Eqs. (18) and (19), to obtain the coefficients a_0 and a_1 of Eq. (4), as

$$S_\lambda = 0.3282 + 240.52/T. \quad (20)$$

Equations (18)–(20) form a consistent set of equations for the calculation of the dilute-gas limit thermal conductivity of *n*-pentane.

The values of the dilute-gas limit thermal conductivity, $\lambda_0(T)$ in mW m⁻¹ K⁻¹, obtained by the scheme of Eqs. (18)–(20), were fitted as a function of the reduced temperature $T_r = T/T_c$ for ease of use to the following equation:

$$\lambda_0(T) = \frac{-3.966\,85 + 35.3805T_r + 5.115\,54T_r^2 - 108.585T_r^3 + 179.573T_r^4 + 39.2128T_r^5}{2.716\,36 - 5.762\,65T_r + 6.778\,85T_r^2 - 0.591\,35T_r^3 + T_r^4}. \quad (21)$$

Values calculated by Eq. (21) do not deviate from the values calculated by the scheme of Eqs. (18)–(20) by more than 0.03% over the temperature range from the triple point to 1000 K. Equation (21) is hence employed in the calculations that will follow.

Figure 21 shows the dilute-gas thermal conductivity values of the selected investigators, and the values calculated by Eqs. (18)–(20), as a function of the temperature. In Fig. 22, percentage deviations of the dilute-gas thermal conductivity of *n*-pentane from the scheme of Eqs. (18)–(20) are also shown.

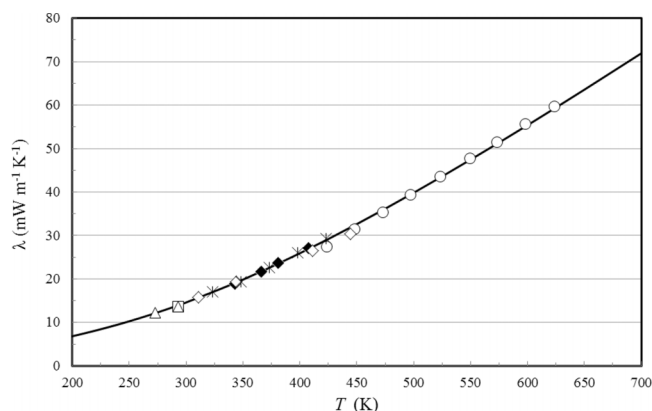


FIG. 21. Dilute-gas thermal conductivity of *n*-pentane as a function of temperature. Dohrn *et al.*⁴⁰ (◆), Naziev *et al.*⁵⁴ (○), Carmichael *et al.*⁶⁵ (◇), Smith *et al.*⁶⁸ (×), Bromley⁶⁹ (□), Moser⁴⁷ (Δ), values calculated by Eq. (21) (—).

They all agree with the present correlation within a maximum deviation of 5%. Based on these measurements, the uncertainty of the correlation, at the 95% confidence level, is 3.8%.

3.3.2. The residual and the critical-enhancement contributions of *n*-pentane

As already mentioned, the coefficients $B_{1,i}$ and $B_{2,i}$ in Eq. (5) were fitted with ODRPACK (Ref. 25) to the primary

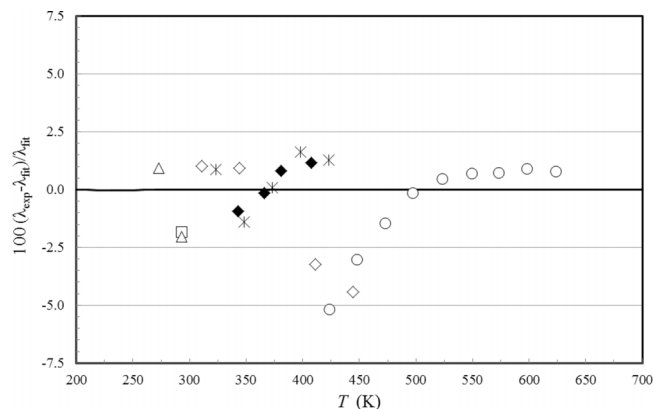


FIG. 22. Percentage deviations of the dilute-gas thermal conductivity of *n*-pentane from the scheme of Eqs. (18)–(20). Dohrn *et al.*⁴⁰ (◆), Naziev *et al.*⁵⁴ (○), Carmichael *et al.*⁶⁵ (◇), Smith *et al.*⁶⁸ (×), Bromley⁶⁹ (□), Moser⁴⁷ (Δ), values calculated by Eq. (21) (—).

TABLE 12. Coefficients of Eq. (5) for the residual thermal conductivity of *n*-pentane

<i>i</i>	$B_{1,i}$ (mW m ⁻¹ K ⁻¹)	$B_{2,i}$ (mW m ⁻¹ K ⁻¹)
1	$7.760\,54 \times 10^{-1}$	$7.976\,96 \times 10^0$
2	$1.176\,55 \times 10^2$	$-7.858\,88 \times 10^1$
3	$-1.331\,01 \times 10^2$	$9.160\,89 \times 10^1$
4	$5.340\,26 \times 10^1$	$-3.704\,31 \times 10^1$
5	$-6.879\,30 \times 10^0$	$5.096\,20 \times 10^0$

data for the thermal conductivity of *n*-pentane. As was done for cyclopentane and *iso*-pentane, we used the values $\Gamma = 0.058$ and $\xi_0 = 2.27 \times 10^{-10}$ m, obtained from the method by Perkins *et al.*²⁷ Furthermore, as in the case of cyclopentane and *iso*-pentane (see Secs. 3.1.2 and 3.2.2), since few data exist in the critical region, see Fig. 20, we estimated the effective cutoff wavelength \bar{q}_D^{-1} using the method of Perkins *et al.*²⁷ and obtained 6.68×10^{-10} m. The viscosity required for Eq. (6) was estimated by an extended corresponding-states method of Huber *et al.*³⁸ The reference temperature T_{ref} was calculated by $T_{\text{ref}} = (3/2) T_c$,³⁹ which for *n*-pentane is 704.55 K. The coefficients $B_{1,i}$ and $B_{2,i}$ of Eq. (5) obtained are shown in Table 12.

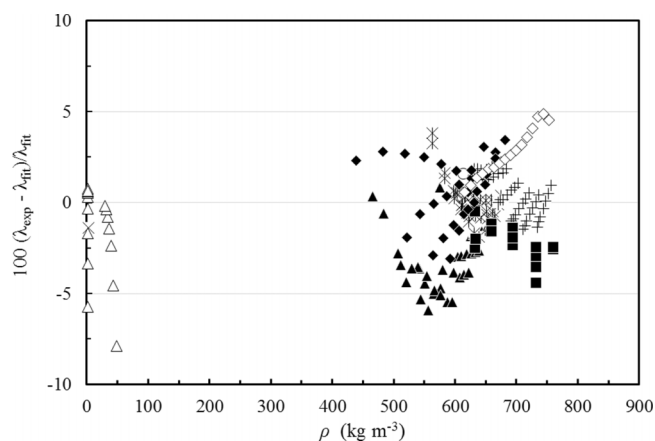
Table 13 summarizes comparisons of the primary data with the correlation. We estimate the uncertainty (at the 95% confidence level) for thermal conductivity from the triple point up to 624 K to be about 3.6% at pressures up to 70 MPa. For the dilute gas, we estimate the uncertainty to be 3.8%. Uncertainties in the critical region are much larger, since the thermal conductivity approaches infinity at the critical point and is very sensitive to small changes in density.

Figure 23 shows the percentage deviations of all primary thermal-conductivity data from the values calculated by Eqs. (1), (5)–(9), and (21), as a function of the density. The lack of experimental data in the critical region is apparent. Figures 24 and 25 show the same deviations, but as a function of the temperature and pressure, respectively.

Table 14 shows the average absolute percentage deviation (AAD) and the bias for the secondary data. Finally, Figs. 26 and 27 show the thermal conductivity of *n*-pentane as a function of the temperature for different pressures, and as a function of the density for different temperatures. The

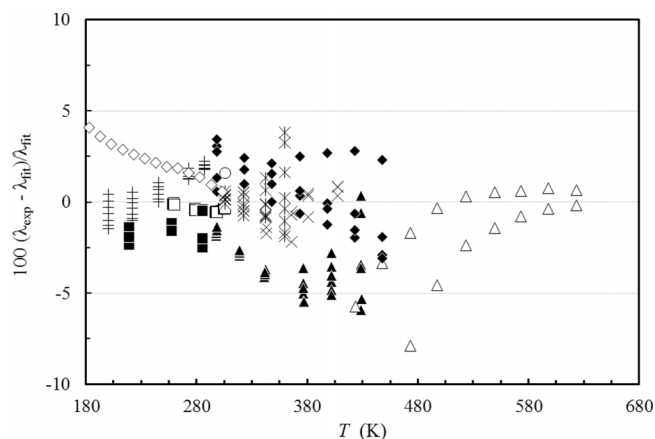
TABLE 13. Evaluation of the *n*-pentane thermal-conductivity correlation for the primary data

First author	Year of publication	AAD (%)	BIAS (%)
Dohrn ⁴⁰	2007	0.92	-0.41
Watanabe ⁴⁹	2003	0.46	-0.46
Watanabe ⁵⁰	2002	0.36	-0.36
Sun ⁵¹	2002	3.32	-3.25
Papadaki ⁵²	1993	1.61	1.61
Palavra ⁵³	1987	1.03	-0.13
Naziev ⁵⁴	1984	1.97	-1.61
Naziev ⁵⁵	1981	0.98	0.45
Kandiyoti ⁵⁶	1972	2.05	2.05
Mukhamedzyanov ⁵⁷	1971	2.19	1.01
Brykov ⁵⁸	1970	2.70	2.70
Entire data set		1.79	0.01

FIG. 23. Percentage deviations of primary experimental data of *n*-pentane from the values calculated by the present model, Eqs. (1), (5)–(9), and (21), as a function of density. Dohrn *et al.*⁴⁰ (×), Watanabe⁴⁹ (●), Sun *et al.*⁵¹ (▲), Watanabe⁵⁰ (□), Papadaki *et al.*⁵² (○), Palavra *et al.*⁵³ (*), Naziev *et al.*⁵⁴ (Δ), Naziev *et al.*⁵⁵ (+), Kandiyoti *et al.*⁵⁶ (■), Mukhamedzyanov *et al.*⁵⁷ (◆), Brykov *et al.*⁵⁸ (◇).

theoretically predicted values of the thermal conductivity around and at temperatures above the critical point are shown.

In Table 15, recommended values for the thermal conductivity are given. As the equation of state of Span and Wagner¹³ is valid up to 70 MPa, we provide recommended values only up to this limit of pressure. For checking computer implementations of the correlation, a point is provided for testing code with critical enhancement at 460 K and 377.687 kg m⁻³ (3.3 MPa), where the thermal conductivity is 71.300 mW m⁻¹ K⁻¹; the dilute-gas thermal conductivity, $\lambda_0(460\text{ K}) = 34.048\text{ mW m}^{-1}\text{ K}^{-1}$, the residual term $\Delta\lambda(377.687\text{ kg m}^{-3}, 460\text{ K}) = 33.325\text{ mW m}^{-1}\text{ K}^{-1}$, and the critical enhancement term, $\Delta\lambda(377.687\text{ kg m}^{-3}, 460\text{ K}) = 3.927\text{ mW m}^{-1}\text{ K}^{-1}$. The viscosity used in the calculation of the enhancement for this state point is 49.465 μPa s.

FIG. 24. Percentage deviations of primary experimental data of *n*-pentane from the values calculated by the present model, Eqs. (1), (5)–(9), and (21), as a function of temperature. Dohrn *et al.*⁴⁰ (×), Watanabe⁴⁹ (●), Sun *et al.*⁵¹ (▲), Watanabe⁵⁰ (□), Papadaki *et al.*⁵² (○), Palavra *et al.*⁵³ (*), Naziev *et al.*⁵⁴ (Δ), Naziev *et al.*⁵⁵ (+), Kandiyoti *et al.*⁵⁶ (■), Mukhamedzyanov *et al.*⁵⁷ (◆), Brykov *et al.*⁵⁸ (◇).

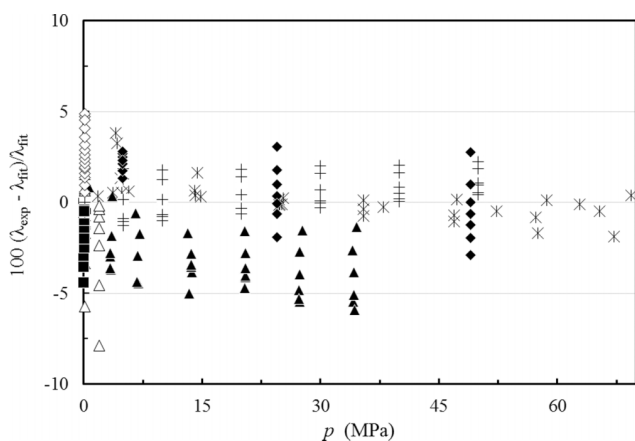


FIG. 25. Percentage deviations of primary experimental data of *n*-pentane from the values calculated by the present model, Eqs. (1), (5)–(9), and (21), as a function of pressure. Dohrn *et al.*⁴⁰ (×), Watanabe⁴⁹ (●), Sun *et al.*⁵¹ (▲), Watanabe⁵⁰ (□), Papadaki *et al.*⁵² (○), Palavra *et al.*⁵³ (*), Naziev *et al.*⁵⁴ (Δ), Naziev *et al.*⁵⁵ (+), Kandiyoti *et al.*⁵⁶ (■), Mukhamedzyanov *et al.*⁵⁷ (◆), Brykov *et al.*⁵⁸ (◇).

TABLE 14. Evaluation of the *n*-pentane thermal-conductivity correlation for the secondary data

First author	Year of publication	AAD (%)	BIAS (%)
Shi ⁵⁹	2006	3.57	−3.57
Heinemann ³¹	2000	8.32	8.32
Rowley ⁶⁰	1987	0.56	0.56
El-Sharkawy ⁶¹	1983	24.5	24.5
Bulanov ⁶²	1974	4.37	4.37
Mallan ⁶³	1972	3.02	3.02
Bogatov ⁶⁴	1969	3.61	−3.61
Carmichael ⁶⁵	1969	5.71	−5.20
Pittman ⁶⁶	1968	2.08	2.08
Jobst ⁶⁷	1964	1.12	0.84
Vilim ⁴⁶	1960	7.18	7.18
Smith ⁶⁸	1960	0.96	0.09
Lambert ³⁶	1955	1.51	−1.51
Bromley ⁶⁹	1952	2.23	−2.23
Riedel ⁷⁰	1948	0.13	0.13
Smith ⁷¹	1936	21.04	21.04
Bridgman ⁷²	1923	11.75	−9.17
Moser ⁴⁷	1913	1.55	1.55
Goldschmidt ⁷³	1911	31.5	−29.1

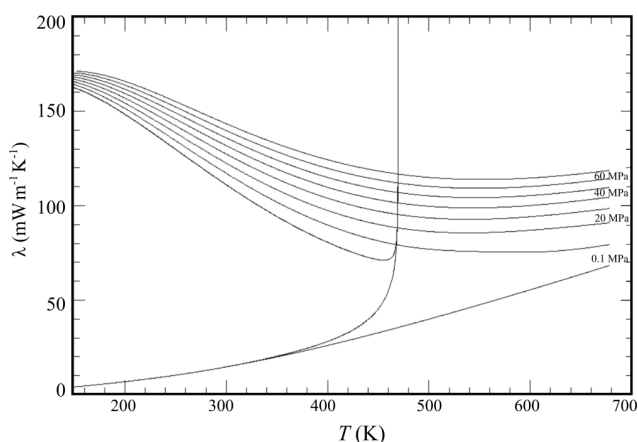


FIG. 26. Thermal conductivity of *n*-pentane as a function of temperature for different pressures.

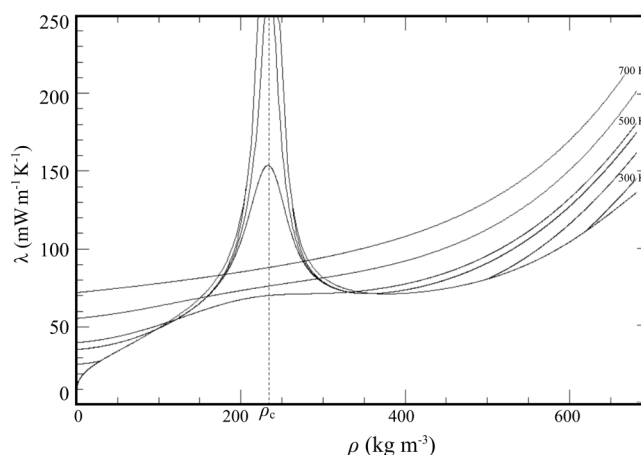


FIG. 27. Thermal conductivity of *n*-pentane as a function of density for different temperatures.

TABLE 15. Recommended values of *n*-pentane thermal conductivity ($\text{mW m}^{-1} \text{K}^{-1}$)

Pressure (MPa)	Temperature (K)			
	200	300	400	500
0	6.83	14.6	25.9	39.9
0.1	148.4	111.1	26.0	39.9
20	154.3	122.4	97.4	86.3
40	159.4	131.7	109.7	99.6
60	163.8	139.7	119.8	110.2
70	165.8	143.4	124.3	114.9

4. Conclusion

New, wide-range reference equations for the thermal conductivity of cyclopentane, *iso*-pentane, and *n*-pentane were presented. The equations are based in part upon a body of experimental data that has been critically assessed for internal consistency and for agreement with theory whenever possible. In the case of the dilute-gas thermal conductivity, a theoretically based correlation was adopted in order to extend the temperature range of the experimental data. In the critical region, the enhancement of the thermal conductivity is well represented by theoretically based equations containing just one adjustable parameter, estimated by a predictive scheme. The thermal-conductivity equations behave in a physically reasonable manner over a wide range of conditions corresponding to the range of validity of the most accurate equations of state for each fluid. The estimated uncertainties of the correlations depend on the availability of accurate experimental data for validation, and are different for each fluid, varying from a low of 1% for the liquid phase of *iso*-pentane over the temperature range $307 \text{ K} < T < 355 \text{ K}$ at pressures up to 400 MPa (where high-accuracy data are available) to a more typical 4% for the liquid phase of cyclopentane over the temperature range $218 \text{ K} < T < 240 \text{ K}$ at pressures to 250 MPa. Estimated uncertainties in the gas phase are typically on the order of 3%–5%. In all three cases, uncertainties in the critical region are much larger, since the thermal conductivity approaches infinity at the critical point and is very sensitive to small changes in density.

Acknowledgment

The authors gratefully acknowledge the partial financial support of the International Union of Pure and Applied Chemistry.

5. References

- ¹M. J. Assael, J. A. M. Assael, M. L. Huber, R. A. Perkins, and Y. Takata, *J. Phys. Chem. Ref. Data* **40**, 033101 (2011).
- ²M. L. Huber, R. A. Perkins, D. G. Friend, J. V. Sengers, M. J. Assael, I. N. Metaxa, K. Miyagawa, R. Hellmann, and E. Vogel, *J. Phys. Chem. Ref. Data* **41**, 033102 (2012).
- ³M. J. Assael, I. A. Koini, K. D. Antoniadis, M. L. Huber, I. M. Abdulagatov, and R. A. Perkins, *J. Phys. Chem. Ref. Data* **41**, 023104 (2012).
- ⁴M. J. Assael, S. K. Mylona, M. L. Huber, and R. A. Perkins, *J. Phys. Chem. Ref. Data* **41**, 023101 (2012).
- ⁵M. J. Assael, E. K. Mihailidou, M. L. Huber, and R. A. Perkins, *J. Phys. Chem. Ref. Data* **41**, 043102 (2012).
- ⁶M. J. Assael, S. K. Mylona, M. L. Huber, and R. A. Perkins, *J. Phys. Chem. Ref. Data* **42**, 013106 (2013).
- ⁷M. J. Assael, I. Bogdanou, S. K. Mylona, M. L. Huber, R. A. Perkins, and V. Vesovic, *J. Phys. Chem. Ref. Data* **42**, 023101 (2013).
- ⁸E. A. Sykioti, M. J. Assael, M. L. Huber, and R. A. Perkins, *J. Phys. Chem. Ref. Data* **42**, 043101 (2013).
- ⁹M. J. Assael, E. A. Sykioti, M. L. Huber, and R. A. Perkins, *J. Phys. Chem. Ref. Data* **42**, 023102 (2013).
- ¹⁰S. K. Mylona, K. D. Antoniadis, M. J. Assael, M. L. Huber, and R. A. Perkins, *J. Phys. Chem. Ref. Data* **43**, 043104 (2014).
- ¹¹H. Gedanitz, M. J. Dávila, and E. W. Lemmon, *J. Chem. Eng. Data* **60**, 1331 (2015).
- ¹²E. W. Lemmon and R. Span, *J. Chem. Eng. Data* **51**, 785 (2006).
- ¹³R. Span and W. Wagner, *Int. J. Thermophys.* **24**, 41 (2003).
- ¹⁴M. J. Assael, M. L. V. Ramires, C. A. Nieto de Castro, and W. A. Wakeham, *J. Phys. Chem. Ref. Data* **19**, 113 (1990).
- ¹⁵R. Hellmann, E. Bich, E. Vogel, and V. Vesovic, *J. Chem. Eng. Data* **57**, 1312 (2012).
- ¹⁶F. R. W. McCourt, J. J. M. Beenakker, W. E. Köhler, and I. Kučšer, *Nonequilibrium Phenomena in Polyatomic Gases* (Clarendon Press, Oxford, 1990).
- ¹⁷B. J. Thijsse, G. W. Thooft, D. A. Coombe, H. F. P. Knaap, and J. J. M. Beenakker, *Physica A* **98**, 307 (1979).
- ¹⁸J. Millat, V. Vesovic, and W. A. Wakeham, *Physica A* **148**, 153 (1988).
- ¹⁹S. Bock, E. Bich, E. Vogel, A. S. Dickinson, and V. Vesovic, *J. Chem. Phys.* **120**, 7987 (2004).
- ²⁰R. Hellmann, E. Bich, E. Vogel, A. S. Dickinson, and V. Vesovic, *J. Chem. Phys.* **130**, 124309 (2009).
- ²¹R. Hellmann, E. Bich, E. Vogel, and V. Vesovic, *Phys. Chem. Chem. Phys.* **13**, 13749 (2011).
- ²²G. A. Olchowy and J. V. Sengers, *Phys. Rev. Lett.* **61**, 15 (1988).
- ²³R. Mostert, H. R. van den Berg, P. S. van der Gulik, and J. V. Sengers, *J. Chem. Phys.* **92**, 5454 (1990).
- ²⁴R. A. Perkins, H. M. Roder, D. G. Friend, and C. A. Nieto de Castro, *Physica A* **173**, 332 (1991).
- ²⁵P. T. Boggs, R. H. Byrd, J. E. Rogers, and R. B. Schnabel, *ODRPACK, Software for Orthogonal Distance Regression, NISTIR 4834, v2.013* (National Institute of Standards and Technology, Gaithersburg, MD, USA, 1992).
- ²⁶G. A. Olchowy and J. V. Sengers, *Int. J. Thermophys.* **10**, 417 (1989).
- ²⁷R. A. Perkins, J. V. Sengers, I. M. Abdulagatov, and M. L. Huber, *Int. J. Thermophys.* **34**, 191 (2013).
- ²⁸H. Watanabe and H. Kato, *J. Chem. Eng. Data* **49**, 809 (2004).
- ²⁹I. M. Marrucho, N. S. Oliveira, and R. Dohrn, *J. Cell. Plast.* **39**, 133 (2003).
- ³⁰M. J. Assael and N. K. Dalaouti, *Int. J. Thermophys.* **22**, 659 (2001).
- ³¹T. Heinemann, W. Klaen, R. Yourd, and R. Dohrn, *J. Cell. Plast.* **36**, 49 (2000).
- ³²B. A. Grigor'ev and A. M. Ishkhanov, *Inzh.-Fiz. Zh.* **41**, 491 (1981).
- ³³P. Andersson, *Mol. Phys.* **35**, 587 (1978).
- ³⁴N. Takada, S. Matsuo, Y. Tanaka, and A. Sekiya, *J. Fluorine Chem.* **91**, 81 (1998).
- ³⁵B. C. Sakiadis and J. Coates, *AIChE J.* **3**, 121 (1957).
- ³⁶J. D. Lambert, K. J. Cotton, M. W. Pailthorpe, A. M. Robinson, J. Scrivins, W. R. F. Vale, and R. M. Young, *Proc. R. Soc. A* **231**, 280 (1955).
- ³⁷H. Preston-Thomas, *Metrologia* **27**, 3 (1990).
- ³⁸M. L. Huber, A. Laesecke, and R. A. Perkins, *Ind. Eng. Chem. Res.* **42**, 3163 (2003).
- ³⁹V. Vesovic, W. A. Wakeham, G. A. Olchowy, and J. V. Sengers, *J. Phys. Chem. Ref. Data* **19**, 763 (1990).
- ⁴⁰R. Dohrn, J. M. Fonseca, R. Albers, J. Kusan-Bindels, and I. M. Marrucho, *Fluid Phase Equilib.* **261**, 41 (2007).
- ⁴¹D. K. Al-Harbi, M. J. Assael, L. Karagiannidis, and W. A. Wakeham, *Int. J. Thermophys.* **12**, 17 (1991).
- ⁴²H. Senftleben, *Z. Angew. Phys.* **17**, 86 (1964).
- ⁴³C. Parkinson and P. Gray, *J. Chem. Soc. Faraday Trans. 1* **68**, 1065 (1972).
- ⁴⁴R. Vilcu and A. Ciocina, *Rev. Roum. Chim.* **17**, 1679 (1972).
- ⁴⁵L. P. Filippov, *Int. J. Heat Mass Transfer* **11**, 331 (1968).
- ⁴⁶O. Vilim, *Collect. Czech. Chem. Commun.* **25**, 993 (1960).
- ⁴⁷E. Moser, Ph.D. thesis, Friedrich-Wilhelms-University, Berlin, 1913.
- ⁴⁸E. W. Lemmon, M. L. Huber, and M. O. McLinden, NIST Reference Fluid Thermodynamic and Transport Properties-REFPROP, version 9.1, National Institute of Standards and Technology, Gaithersburg, MD, 2013, <http://www.nist.gov/srd/nist23.cfm>.
- ⁴⁹H. Watanabe, *J. Chem. Eng. Data* **48**, 124 (2003).
- ⁵⁰H. Watanabe, *Int. J. Thermophys.* **23**, 337 (2002).
- ⁵¹L. Sun, J. E. S. Venart, and R. C. Prasad, *Int. J. Thermophys.* **23**, 391 (2002).
- ⁵²M. Papadaki, M. Schmitt, A. Seitz, K. Stephan, B. Taxis, and W. A. Wakeham, *Int. J. Thermophys.* **14**, 173 (1993).
- ⁵³A. M. F. Palavra, W. A. Wakeham, and M. Zalaf, *Int. J. Thermophys.* **8**, 305 (1987).
- ⁵⁴Y. M. Naziev, A. M. Gumbatov, and A. K. Akhmedov, *Izv. Vyssh. Uchebn. Zaved., Neft Gaz* **53** (1984).
- ⁵⁵Y. M. Naziev, A. M. Gumbatov, and A. K. Akhmedov, *Izv. Vyssh. Uchebn. Zaved., Neft Gaz* **43** (1981).
- ⁵⁶R. Kandiyoti, E. McLaughlin, and J. F. T. Pittman, *J. Chem. Soc. Faraday Trans. 1* **68**, 860 (1972).
- ⁵⁷I. K. Mukhamedzyanov, G. K. Mukhamedzyanov, and A. G. Usmanov, *Trudy Kazan. Khim. Teknol. In-ta* **47**, 22 (1971).
- ⁵⁸V. P. Brykov, G. K. Mukhamedzyanov, and A. G. Usmanov, *Inzh.-Fiz. Zh.* **18**, 62 (1970).
- ⁵⁹Y. Shi, L. Sun, J. E. S. Venart, and R. C. Prasad, *J. Therm. Anal. Calorim.* **86**, 585 (2006).
- ⁶⁰R. L. Rowley and G. L. White, *J. Chem. Eng. Data* **32**, 63 (1987).
- ⁶¹A. A. El-Sharkawy, M. A. Kenawy, and A. Z. Dakrouy, *High Temp. - High Pressures* **15**, 391 (1983).
- ⁶²N. V. Bulanov, E. D. Nikitin, and V. P. Skripov, *J. Eng. Phys. Thermophys.* **26**, 136 (1974).
- ⁶³G. M. Mallan, M. S. Michaelian, and F. J. Lockhart, *J. Chem. Eng. Data* **17**, 412 (1972).
- ⁶⁴G. F. Bogatov, Ph.D. thesis, *Izv. vyssh. ucheb. Zaved., Neft'i Gaz*, 1969.
- ⁶⁵L. T. Carmichael, I. Jacobs, and B. H. Sage, *J. Chem. Eng. Data* **14**, 31 (1969).
- ⁶⁶J. F. T. Pittman, Ph.D. thesis, Imperial College of Science and Technology, London, 1968.
- ⁶⁷W. Jobst, Ph.D. thesis, Techn. Hoch., Zurich, 1964.
- ⁶⁸W. J. S. Smith, L. D. Durbin, and R. Kobayashi, *J. Chem. Eng. Data* **5**, 316 (1960).
- ⁶⁹L. A. Bromley, Ph.D. thesis, University of California, Berkeley, 1952.
- ⁷⁰L. Riedel, Ph.D. thesis, Technischen Hochschule Friderician, Karlsruhe, 1948.
- ⁷¹J. F. D. Smith, *Trans. Am. Soc. Mech. Eng.* **58**, 719 (1936).
- ⁷²P. W. Bridgman, *Proc. Am. Acad. Arts Sci.* **59**, 141 (1923).
- ⁷³R. Goldschmidt, *Physik Z.* **12**, 417 (1911).
- ⁷⁴M. Jaeschke and P. Schley, *Int. J. Thermophys.* **16**, 1381 (1995).